Food Chemistry 192 (2016) 660–667

Contents lists available at ScienceDirect

Food Chemistry

journal homepage: www.elsevier.com/locate/foodchem

The influence of cheese composition and microstructure on the diffusion of macromolecules: A study using Fluorescence Recovery After Photobleaching (FRAP)

A.L. Chapeau [a], Juliana V.C. Silva [a], Pierre Schuck [a], Anne Thierry [a], Juliane Floury [a,b,*]

[a] INRA, UMR1253, Science and Technology of Milk and Eggs, F-35042 Rennes Cedex, France
[b] AGROCAMPUS OUEST, UMR1253, Science and Technology of Milk and Eggs, F-35042 Rennes Cedex, France

ARTICLE INFO

Article history:
Received 13 March 2015
Received in revised form 8 July 2015
Accepted 10 July 2015
Available online 11 July 2015

Keywords:
Cheese
Fluorescence Recovery After Photobleaching (FRAP)
Microstructure
Water
Ripening

ABSTRACT

In cheese technology, the diffusion phenomena are crucial during ripening. The technique of Fluorescence Recovery After Photobleaching was applied for the first time on real cheese, in order to investigate the relationships between molecular diffusion and the cheese composition and/or its microstructure. Measured effective diffusion coefficients in soft and hard cheese of a group of dextrans (10–500 kDa) were found to be in the same order of magnitude with values observed when using a comparable non-fat model cheese (~0.1–20 $\mu m^2 s^{-1}$). Diffusion of the dextrans was mainly dependent on the fraction of "free" aqueous phase present in the cheese, closely which is linked to cheese-making technology and ripening stage. Diffusion coefficients were modeled by a power law relationship as a function of dextran molecular weight, which allowed some study of the cheese microstructure. A tighter protein network will require some deformation of those flexible macromolecules with a higher molecular weight (>250 kDa), in order to diffuse through the pores of such cheese structures.

© 2015 Elsevier Ltd. All rights reserved.

1. Introduction

Molecular diffusion, as characterized by diffusion coefficients, is a key feature in the manufacture of certain food products, especially those from the dairy industry. During the manufacture of cheese, the coagulation of caseins forms a protein gel structure that entraps the aqueous phase of milk (whey proteins, minerals...), fat and micro-organisms. Cheese ripening involves complex microbiological and biochemical reactions that take place within this protein gel resulting in the development of flavor and texture characteristics, specific to each cheese variety (McSweeney, 2004). Such protein gel structure (also referred to as a protein network) acts like a sieve, where the gel strands impedes the diffusing molecules; a denser gel structure leading to a greater obstruction (Aly et al., 2011; Floury, Madec, Waharte, Jeanson, & Lortal, 2012; Jeanson et al., 2011).

For polymer gels, a simple power law model, developed by De Gennes (1979) (which is based on the principle of hydrodynamic interactions between the diffusing molecules and the gel matrix), can be applied to describe the diffusion behavior of flexible macromolecules as a function of their molecular weight (Eq. (1)):

$$D_{eff} = A \cdot MW^{-\alpha} \quad (1)$$

where D_{eff} is the effective diffusion coefficient of the macromolecule in the gel ($\mu m^2 s^{-1}$), A is a constant, MW is the molecular weight of the macromolecule and α is a characteristic exponent (Favre, Leonard, Laurent, & Dellacherie, 2001). Depending on the value of the exponent α, this model enables the identification of the diffusion regime in the gel (Tao, Lodge, & von Meerwall, 2000) consequently enabling useful features of the gel microstructure, such as its pore size to be determined (Favre et al., 2001). When $0.5 < \alpha < 0.6$, the diffusing solutes behave as "ideal spheres" in a very dilute system (De Gennes, 1979), implying that they have enough space to diffuse in between the pores of the gel matrix without modifying their shape. If the solute molecule diameter approaches the gel pore size, an intermediate stage occurs with an α value close to 1, which corresponds to a situation in which solutes take on an ellipsoidal shape. In even more highly concentrated polymer systems, the gel pore size decreases further, forcing any diffusing flexible macromolecular solute to adopt a "wormlike" behavior in order to move: this corresponds to an α value close to 2. The solutes are otherwise too large to enter the pores of the gel

* Corresponding author at: INRA, UMR1253, Science and Technology of Milk and Eggs, F-35042 Rennes Cedex, France.
E-mail address: Juliane.Floury@agrocampus-ouest.fr (J. Floury).

http://dx.doi.org/10.1016/j.foodchem.2015.07.053
0308-8146/© 2015 Elsevier Ltd. All rights reserved.

structure and have thus to change their shape in order to diffuse which is also referred as the reptation mode (De Gennes, 1979).

Floury, Jeanson, Aly, and Lortal (2010) reported a significant lack of published data on diffusion coefficients of macromolecular solutes in cheese, most of the existing papers dealing only with the diffusion of NaCl and small solutes during the salting and ripening processes. They also noted that most diffusion coefficients for these solutes were obtained from a method based on spatio-temporal concentration profiles, which has the drawback of being macroscopic, destructive and time-consuming.

The alternative approach of Fluorescence Recovery After Photobleaching (FRAP), coupled to a confocal scanning laser microscope (CSLM), was recently developed to determine effective diffusion coefficients of labeled macromolecules in a model cheese (Floury et al., 2012; Silva, Peixoto, Lortal, & Floury, 2013).This technique is non-destructive and has a good spatio-temporal resolution, unlike the established method which is based on concentration profiles. The model cheese was made from a fat-free dairy gel obtained from an ultrafiltered milk protein concentrate. The use of such a standard formulation ensured a homogeneous microstructure, facilitating the application of the FRAP technique. Effective diffusion coefficients (D_{eff}) of dextrans and dairy proteins labeled with fluorescein isothiocyanate, chosen because of their different physicochemical properties of size, shape and charge, have been successfully measured using FRAP in the model cheese (Silva et al., 2013). Dextran macromolecules from 4 to 2000 kDa could diffuse through the model cheese, even if their diffusion coefficients within the protein network were reduced relative to that in water. Silva et al. (2013) also observed that the decrease of the diffusion coefficients of dextran molecules as function of their molecular weight could be modeled by a power law relationship with an exponent of −0.5. It was deduced from these results that the pore sizes of the model cheese were much larger than the diameter of the largest dextran molecule studied. This hypothesis was confirmed by image analysis of the microstructure of the model cheese obtained by transmission electron microscopy (Silva, Legland, Cauty, Kolotuev, & Floury, 2015). In this study, a protocol involving high pressure freezing coupled with a freeze-substitution was applied prior to transmission electron microscopy to minimize any modification of the microstructure of the cheese sample. The mean pore size in the cheese was demonstrated to be much larger (≈150 nm) than the hydrodynamic diameter of the larger diffusing dextran molecule (≈50 nm).

The objective of the present work is to determine how the diffusion phenomena of macromolecules are influenced by the composition and/or microstructure of commercially available cheese. Diffusion coefficients of a range of dextrans (10–500 kDa) were measured in different cheese varieties including soft and hard cheeses, with different ripening times. Their composition and "free" water content were measured, and separately, their microstructure was analyzed by confocal microscopy by specific fluorescent labeling of proteins and fat.

2. Material and methods

2.1. Manufacture of cheeses

Raw bovine milk was purchased from a local dairy and stored at 4 °C until use. The milk was first pasteurized at 74 °C for 20 s, skimmed at 50–55 °C and then microfiltered (1.4 μm pore size membrane) to remove the residual micro-organisms and somatic cells (Ulve et al., 2008). The cream was heat-treated for 20 s in a current flow tube electric heat exchanger (Actijoule®, Actini Group, Evian-les-Bains, France) to 95 °C or 120 °C, for the soft and hard cheeses, respectively.

2.1.1. Soft cheese (Camembert-type)

Pasteurized cream was added to a 60 L batch of microfiltered skimmed milk to obtain the standardized milk with adjusted protein and fat contents of 33.5 and 32 g kg^{-1}. Freeze-dried, mixed-mesophilic starter cultures of *Lactococcus lactis* MM100 (5DCU·100 L^{-1}) and *Geotrichum candidum* GEO 17 (2DCU·1000 L^{-1}), *Penicillium camemberti* LV2 (5DCU·1000 L^{-1}), *Kluyveromyces lactis* 71 suspensions (2DCU·1000 L^{-1}), each prepared according to the manufacturer's instructions (Danisco-Dupont, Dangé Saint-Romain, France), were added to the milk and mixed in thoroughly. After the addition of the cultures, the milk samples were held for 18 h at 12 °C to develop acidity reaching pH 6.3. An aliquot of liquid microbial rennet (Chymax plus 200 IMCU·mL^{-1}Chr. Hansen, Arpajon, France) was diluted 1:10 in distilled water and immediately added to the acidified milk (previously heated up to 35 °C) and mixed in thoroughly to give a final concentration of 0.20 mL L^{-1}.The mixture was then incubated for a further 40 min at 32–33 °C to enable coagulation. The produced curd was then cut into 2 cm cubes, and carefully transferred into circular open molds (20 cm in diameter and 9 cm high, with drainage holes in the sides) and allowed to drain for 1.5 h at 26 °C. The curd was turned and drained after 45 min, 2 h and 5 h, and then left for a further 18 h at 18 °C. After draining, the curd was removed from the molds and immersed in brine (35% NaCl) for 25 min at 12 °C.

Two samples of cheese before ripening (denoted as Day 1) were withdrawn (one before brining and one after brining), then packed under vacuum in semi-permeable and thermo-retractable ripening bags (BK1L, Cryovac, Epernon, France) and placed at 4 °C to be used within the following 48 h for chemical characterization, microstructural determination and in the FRAP procedure.

The remainder of the cheese was placed in a ripening room (12 °C, 97% relative humidity (RH)) for 15 days and turned every 3 days before analysis (these samples being denoted as Day 15).

2.1.2. Hard cheese (Swiss-type)

Samples of this type of cheese were previously manufactured as part of the European FP7 TeRiFiQ project. Pasteurized cream was added to a 60 L batch of microfiltered skimmed milk to obtain the standardized milk with adjusted protein and fat contents of 33.4 and 29.6 g kg^{-1}. This milk was supplemented with a 47 w/w% $CaCl_2$ solution (20 mL 100 L^{-1}; Maxical, Chr. Hansen, Arpajon, France), then warmed to 32 °C and inoculated with starters: (i) 0.12vol/vol% of a culture of *Streptococcus thermophilus* (PALITG ST88, Laboratoires Standa, Caen, France) grown at 42 °C for 4 h on Marstar 412 A medium (Danisco-Dupont, Dangé Saint-Romain), (ii) 0.1 vol/vol% of a culture of *Lactobacillus helveticus* (CIRM-BIA103, Centre International de Ressources Microbiennes-Bactéries d'IntérêtAlimentaire, INRA, Rennes, France) grown on PhagexLb medium (LaboratoiresStanda) at 42 °C for 6 h, and (iii) 1 g of freeze-dried/100 L of freeze dried *Propionibacterium freudenreichii* (PALITGP20); Laboratoires Standa). The milk was then held for 30 min at 32 °C (pH 6.6) before adding liquid microbial chymosin (Chymax plus 200 IMCU·mL^{-1}) at a final concentration of 0.20 mL L^{-1}. The milk mixture was further incubated at 32 °C until the curd was sufficiently firm to be cut in 2–3 cm cubes. Curd pieces were heated to 53 °C for 35 min, then placed into stainless steel macro-perforated molds for pre-pressing at 10 g cm^{-2}, and then allowed to drain for 30 min. The pre-pressed curd was cut into five blocks of 2 kg each, and placed in micro-perforated plastic molds (18 cm diameter) for pressing at 100 g cm^{-2} for 1 h in a room at 35 °C and 90% RH. These were then held for 3 h at 45 °C and then 16 h at 35 °C, to enable acidification. The cheese was taken out of the mold and cooled in a room at 13 °C for 4 h. The cheese blocks were salted by immersion in baths of stirred saturated brine at 12 °C: the process ended when the salt content of

the cheese reached 1% w/w. Cheese samples were soaked with a 1000 ppm natamycin solution (Mycopim, Laboratoires Standa, Caen, France) before being packed under vacuum in semi-permeable and thermo-retractable ripening bags (BK1L, Cryovac, Epernon, France).

A cheese block was withdrawn before ripening (sample denoted as Day 1), and placed at 4 °C to be analyzed within the following 48 h for FRAP measurements, cheese composition, and microstructural study.

The other cheese blocks were placed in a ripening room (97% relative humidity) at 12 °C for 20 days and then at 23 °C for 18 days. One block was withdrawn for analyze after 8 days of ripening (Day 8) and a second at the end of the ripening time (Day 48): both were held at 4 °C to be analyzed within the following 48 h.

2.2. Cheese composition

2.2.1. Moisture content

Dry matter content (DM, %) was measured following the International Dairy Federation reference method (1987). Total moisture content (%) is 100-DM.

2.2.2. Fat content

(*F*, %) was determined using the Van Gulikbutyrometric method (International Dairy Federation, 1986).

2.2.3. Free moisture in non-fat cheese

The "free" water fraction was measured by the desorption of water at 20 °C (the temperature at which the FRAP measurements were also performed), through an adaptation of the method initially developed by Schuck et al. (2009) for concentrated milk. A 0.5 g sample of cheese was dried at 20 °C (±1 °C) in an air-sealed vessel for 72 h. The drying apparatus (Rotronic, Bassersdorf, Switzerland) comprised a compartment cell containing the sample which was placed above a cylindrical steel cell filled with zeolite. A gradient of partial pressure was then created from the cheese sample to the zeolite, causing the desorption of water from the sample. The variation of the relative humidity (*RH*) of the air in the cell was measured during desorption by a humidity sensor outputting to a computer. Analysis of the *RH* kinetics using the SD2P® software (INRA, France) enabled the determination of the water fraction that is "easily" transferred from the sample to the zeolite, referred to in the present study as the "free water fraction".

Cheese makers and scientists in the field usually give the percentage of moisture on a fat-free basis, which serves to characterize the protein matrix in which fat is embedded. This measurement defines the cheese category (soft, semi-hard, hard cheeses), independently of the level of fat (full or reduced-fat cheese) (Mahaut, Jeantet, and Brulé, 2000). This parameter is defined as:

$$\frac{\text{Total water content (\%)}}{100-\text{fat (\%)}} = \frac{100-\text{dry matter (\%)}}{100-\text{fat (\%)}} \quad (2)$$

By knowing the "free water fraction" of the total water content of the cheese, a new parameter called "free moisture in non-fat cheese" was defined as:

$$\text{FM in non}-\text{fat cheese (\%)} = \frac{100-\text{DM}}{100-F} \times \text{free water fraction} \quad (3)$$

All these analyses were performed in triplicate for each soft and hard cheese sample obtained at each ripening time, respectively denoted as:

- soft cheese Day 1 before brining, Day 1 after brining and Day 15;
- hard cheese Day 1, Day 8 and Day 48.

2.2.4. Microstructural analysis

Thin slices, measuring approximately 5 × 5 × 2 mm thick, were cut from the heart of the cheese using a scalpel. The protein network and fat components were stained using fluorescent dyes (Sigma–Aldrich, St Louis, USA): 5 μL of a 10% Fast Green aqueous solution and 10 μL of a 0.1% Nile Red propanediol solution were deposited on the surface of the slice. The sample was held at 4 °C for 30 min to permit the diffusion of the fluorescent dyes into the cheese curd. The sample was then set between glass slides for observation by an 100× objective lens (oil immersion) of an inverted Confocal Laser Scanning Microscope (CLSM) (Nikon, Champigny-sur-Marne, France) using 543 and 632 nm excitation wavelengths in dual-beam fluorescent mode for fat and protein detection, respectively. Micrographs had a resolution of 1024 × 1024 pixels. The depth of optical sectioning depended on the optical density of the samples (varying from 100 to 350 mm from the surface of the sample). There were at least two samples of each cheese type, and for each sample at least 5 micrographs were taken. For the double-stained samples, the protein network was coded in green and the fat phase in red. The aqueous phase appeared as black zones in the confocal micrographs.

2.3. Diffusion measurements

2.3.1. Diffusing macromolecules

Dextrans of 6 different MW between 10 and 500 kDa were purchased from Sigma–Aldrich (St. Louis, MO, USA). These were tagged with fluorescein isothiocyanate conjugate and denoted as D10, D20, D40, D70, D150, D250, and D500 according to their nominal average MW. Diffusion coefficients of these FITC-dextrans in milk aqueous phase (permeate from the milk ultrafiltration) (D_{aq}) have been previously determined using the FRAP procedure at 19 °C (Silva et al., 2013). This solution, mainly composed of water, lactose and minerals, was used to represent the continuous aqueous phase filling the voids of cheeses. The hydrodynamic radii (R_h) of each dextran molecule were calculated from the corresponding diffusion coefficients using the Stokes–Einstein relation (Eq. (3)).

$$D_{aq} = \frac{k_B T}{6\pi\eta_{aq} R_h} \quad (4)$$

where k_B is the Boltzmann's constant (1.38×10^{-23} J K^{-1}), η_{aq} is the viscosity of the aqueous phase (given as 1.2 mPa (Bouchoux, Gésan-Guiziou, Pérez, & Cabane, 2010)) and T is the absolute temperature (K).

The MW, D_{aq} and R_h values of each FITC-dextran are summarized in Table 1.

Table 1
Molecular weights (MW) and diffusion coefficients in the cheese aqueous phase (D_{aq}) of FITC-dextrans (D10–D500), at 19 °C and their corresponding hydrodynamic radii (calculated R_h).

FITC-dextrans	MW (kDa)	D_{aq}[a] (μm^2 s^{-1})	R_h[b] (nm)
D10	10	60 ± 3.8	3.0 ± 0.2
D20	20	40 ± 2.8	4.5 ± 0.3
D40	40	34 ± 2.0	5.2 ± 0.3
D70	70	26 ± 1.6	6.9 ± 0.4
D250	250	23 ± 2.3	7.7 ± 0.8
D500	500	11 ± 0.7	16.2 ± 1.1

[a] Diffusion coefficient in the cheese aqueous phase at 19 °C determined by Fluorescence Recovery After Photobleaching (data from Silva et al. (2013)). Diffusion coefficients are given as mean ± standard deviation for 10 acquisitions.
[b] Hydrodynamic radius of solutes calculated from the Stokes–Einstein equation (Eq. (3)).

2.3.2. FRAP analysis

The FRAP technique was carried out using a CSLM for measuring the effective diffusion coefficients (D_{eff}) of the FITC-dextrans within the protein network of the different cheese types at different ripening times. The samples were observed using a 40× objective lens (oil immersion) with a numerical aperture of 1.30. A thin slice of cheese was cut and 5 μL of the FITC-dextran solution was placed on its surface. The sample was held at 4 °C for 30 min to permit the diffusion of the FITC-dextran molecules into the cheese matrix. The sample was then set between glass slide and cover slip for the FRAP procedure, performed at 20 °C in an air-conditioned room, following the protocol described in Silva et al., 2013. In summary, this involved taking, confocal micrographs at a constant depth of 15 μm from the coverslip. The FITC-dextrans were excited using a 50 mW sapphire laser system at a wavelength of 488 nm and detected on a 500–530 nm spectral bandwidth. The image size was fixed to 256 × 256 pixels with a pixel of 1.24 μm. The bleached spot, or Region Of Interest (ROI), was 10.4 μm in diameter. As shown in Fig. 1 (Supplementary material), the position of the ROI has been chosen in order to only photobleach the protein network, and over a sufficiently large and homogeneous region to be able to further extract the profile width in the radial direction from image processing routines as described in Floury et al. (2012). Each FRAP measurement started with the acquisition of 3 image scans acquired at 0.1% of the maximum laser intensity, followed by a bleach pulse of 5 image scans at 100% intensity on a ROI spot with a 5.2 μm radius. Depending on the solute molecule size, a series of 50–200 single-section images, were then collected at 480 ms intervals and with 0.1% of the maximum laser intensity, to monitor the recovery process. Data were analyzed by using the diffusion model of Braga, Desterro, and Carmo-Fonseca (2004). A strength of this model is that it takes into account the diffusion of the solutes during the photobleaching phase and before the acquisition of first image of the recovery phase (Floury et al., 2012). Analyses of the recorded images were carried out using the EZ-C1 Free Viewer 300 software, Gold Version 3.2, (Nikon Corporation, Tokyo, Japan).

For each cheese sample, twelve FRAP acquisitions were carried out to enable a reliable average value of D_{eff} for each FITC-dextran.

2.4. Statistical analysis

The mean values of effective diffusion coefficients obtained for each FITC-dextran in the different cheese samples and their respective mean values of composition (moisture, fat and free moisture in non-fat cheese content) were statistically compared using R software. One-way analysis of variance (ANOVA) and Fishers' Least Significant Difference (LSD) test were applied in order to determine which mean values were significantly different at the 95% family-wise confidence level. The Pearson correlation coefficients were calculated to get a measure of the linear dependence between the mean values of the diffusion coefficients of the solutes (D10, D20, D40, D70 and D500) measured in the different samples of cheese (different type of cheeses and ripening times) and the respective composition variables of the samples (fat content, moisture content and free moisture in non-fat cheese).

3. Results

3.1. Composition and microstructure of cheeses

Table 2 presents the mean composition values of the different cheeses studied throughout ripening. Whereas the previously studied model cheese contained no fat, the soft and hard cheeses of this study contained around 21% and 30% of fat, respectively. Fat content were constant throughout the ripening process in both types of cheese. With respect to moisture and free moisture in non-fat cheese contents, significant differences were measured between each cheese sample. The model cheese contained the highest moisture and FM in non-fat cheese contents, whereas the hard cheese samples displayed the lowest values for both parameters, and the soft cheese was in between. Neither moisture nor FM in non-fat cheese contents varied significantly during the ripening of the hard-cheese, unlike the soft cheese for which both values significantly fell after 15 days of ripening. No significant difference could be discerned between soft cheese samples before and after brining at Day 1. The FM in non-fat cheese content of soft cheese after 15 days of ripening was of the same order of magnitude as the hard cheese.

Table 2
Composition of model, soft and hard cheeses, at different ripening times. Values are given as a mean ± one standard deviation (based on 3 replicates). Different letters for mean values correspond to significant differences at $p < 0.05$.

Cheese	Ripening day	Fat content (%)	Moisture content (%)	Free moisture in non-fat cheese (%)
Model	0	0	$77.8^{a} \pm 0.1$	75^{a}
Soft	1 (before brining)	21 ± 0.1	$58.8^{b} \pm 0.2$	$64^{a} \pm 2.2$
	1 (after brining)	21 ± 0.1	$57.2^{b} \pm 0.2$	$62^{a} \pm 0.1$
	15	21 ± 0.1	$41.4^{bc} \pm 0.1$	$37^{b} \pm 1.9$
Hard	1	29.6 ± 0.1	$36.7^{c} \pm 0.1$	$29^{b} \pm 2.9$
	8	29.8 ± 0.1	$35.4^{c} \pm 0.1$	$26^{b} \pm 1.1$
	48	29.8 ± 0.1	$36.3^{c} \pm 0.1$	$29^{b} \pm 0.8$

The results are expressed as the mean ± one standard deviation of the mean ($n = 3$).

Fig. 1 presents the confocal micrographs of soft and hard cheeses before and after ripening. For the soft cheese at Day 1, Fig. 1A shows that the protein network was not completely formed and individual curd grains were not fully fused. Fat was dispersed within this protein network as large almost spherical globules. Large and numerous black zones were visible in the protein network, corresponding to whey serum pockets. This corresponds to the aqueous phase of the cheese, but also contains more of the less soluble whey proteins of milk, depending of the cheese technology used. After 15 days of ripening, the curd grains were finally fused together, forming a continuous homogeneous protein network (Fig. 1B). Within this network, it can be noticed that the fat globules have aggregated during the ripening process, forming a lipid network resulting from the coalescence of globules. Black zones were much fewer, indicating that the cheese curd had lost the largest part of its whey serum phase during ripening.

As shown by Fig. 1C–E, the hard cheese samples exhibit a continuous protein network even before ripening. Compared to the soft cheese this network appeared much denser throughout the ripening process. Fat did not appear as globules but more like elongated inclusions within the protein network, due to the coalescence of fat globules during the heating and pressing process of the curd after molding. Large pockets of whey serum were observed before the ripening process (Fig. 1C), but they were absent after 8 days (Fig. 1D) and 48 days (Fig. 1E).

3.2. Diffusion behavior of dextrans in cheese

Fig. 2 presents logarithmic plots of effective diffusion coefficients (D_{eff}) of the FITC-dextrans obtained by the FRAP technique for the different cheeses studied throughout ripening. Effective diffusion coefficients previously obtained by Silva et al. (2013) in a model cheese are also plotted on the Fig. 2 for comparison. Values of effective diffusion coefficients of FITC-dextrans obtained by FRAP in real soft or hard cheeses were in the same order of magnitude compared with the model cheese. Moreover, the variation

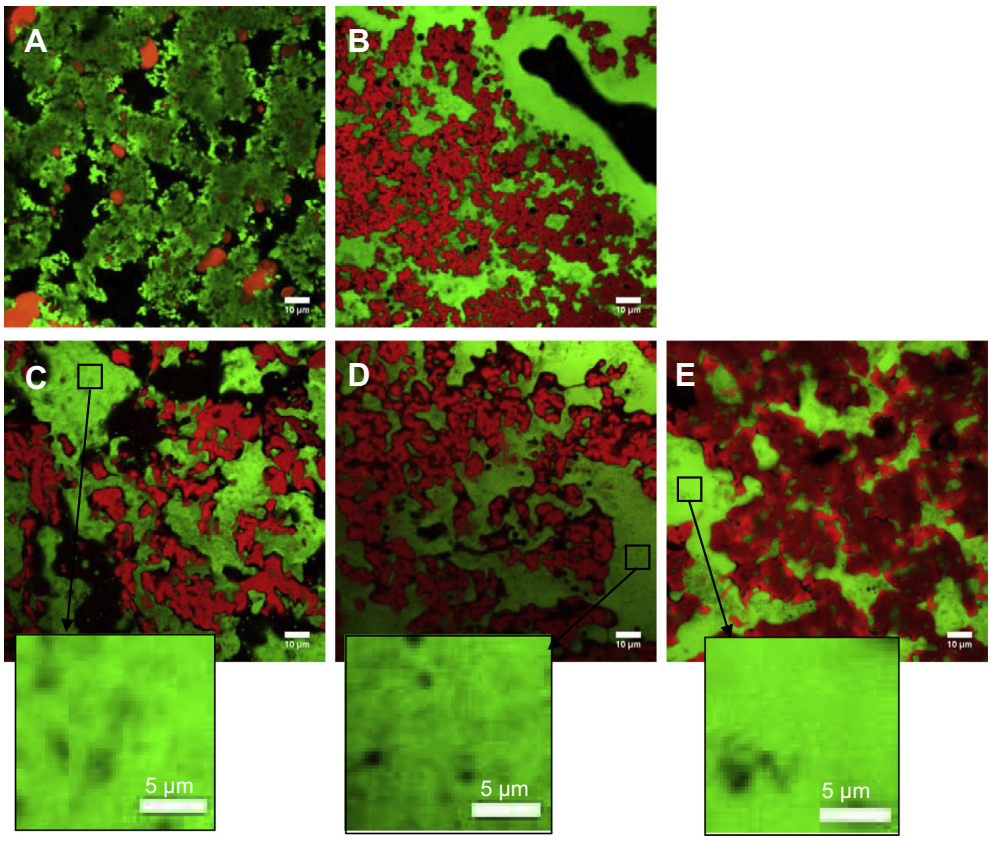

Fig. 1. Confocal laser scanning micrographs of cheeses. (A) Soft cheese Day 1 before brining, (B) soft cheese Day 15. (C) hard cheese Day 1, (D) hard cheese Day 8, (E) hard cheese Day 48. The fat is coloured in red, the protein network in green, and black zones correspond to the aqueous phase. (For interpretation of the references to colour in this figure legend, the reader is referred to the web version of this article.)

of D_{eff} with the molecular weight (MW) of the dextran solute up to 250 kDa, followed a decreasing power law relationship (Eq. (1)) in all cheeses except in the hard cheese at Day 1. Table 3 gives the corresponding fitted A and α parameters obtained from this power law model for each cheese sample. High coefficients of determination (R^2) were obtained. The characteristic exponent α varied little irrespective of the cheese matrix and the ripening time, with values falling in the range 0.5–0.6 for FITC-dextrans from 10 to 250 kDa. However, while this power law relationship was still valid up to the large dextran molecules (500 kDa) both in the model and non-ripened soft cheeses, a strong fall of the effective diffusion coefficient of 500 kDa dextran in the soft cheese at Day 15 and in all hard cheese samples was observed. On the other hand, it is noteworthy that the values for the constant A were dependent both on the type of cheese and the ripening time. In the cheese with the highest humidity, such as the model and soft cheese, the A values were much higher before ripening (between 75 and 123) than after ripening (around 40), with a reduction by a factor 3. For the hard cheese, A remained almost constant during ripening with values close to 40 both at Day 8 and 48. For the hard cheese at Day 1 (before ripening), the effective diffusion coefficient of the two smallest dextran molecules (10–20 kDa) were close to the values obtained in the model and soft cheese before ripening, whereas values of the largest dextran molecules (from 40 to 500 kDa) were more similar to those obtained for the other hard cheese samples at Day 8 and Day 48.

3.3. Correlations between effective diffusion coefficients of dextrans and the cheese composition

Table 4 sets out the correlation coefficients between the effective diffusion coefficients of each FITC-dextran (D10, D20, D40, D70 and D500) and the composition variables of the cheese (fat content, moisture content, free moisture in non-fat cheese). Values for the correlation coefficients between D_{eff} and the cheese fat content were very low irrespective of the dextran. Conversely, the correlation coefficients were particularly good (close to 0.9) for the diffusion coefficients and *FM* in non-fat cheese contents, especially for the FITC-dextrans between 40 kDa and 500 kDa. The correlation between the effective diffusion coefficients of dextrans and the moisture contents was slightly lower at around 0.7. The interpretation of these results is that the effective diffusion coefficient of the dextrans depended more on the *FM* in non-fat cheese content, (i.e. the "free" water fraction actually available for the diffusion of the solute molecules within the cheese matrix), than on the total water content of the cheese.

4. Discussion

A soft and a hard cheese were chosen in order to explore diffusion phenomena in cheese as a function of both different production technology and ripening duration. This approach enabled the study of differences in composition and microstructure of the cheese, especially with respect to the free moisture in non-fat phase of the cheese. All of the results produced here were compared to the study of Silva et al. (2013) carried out on a model cheese based on the rennet coagulation of ultrafiltered non-fat milk. This standardized cheese had a homogenous protein network whose microstructure was fully characterized by Silva et al. (2015).

The power law equation linking D_{eff} and *MW* of dextrans (Eq. (1)) used to model the data enabled (i) the comparison of diffusion behaviors of dextrans in matrices obtained from different cheese-making technologies and (ii) to relate them to the composition and microstructure of these same cheeses during ripening.

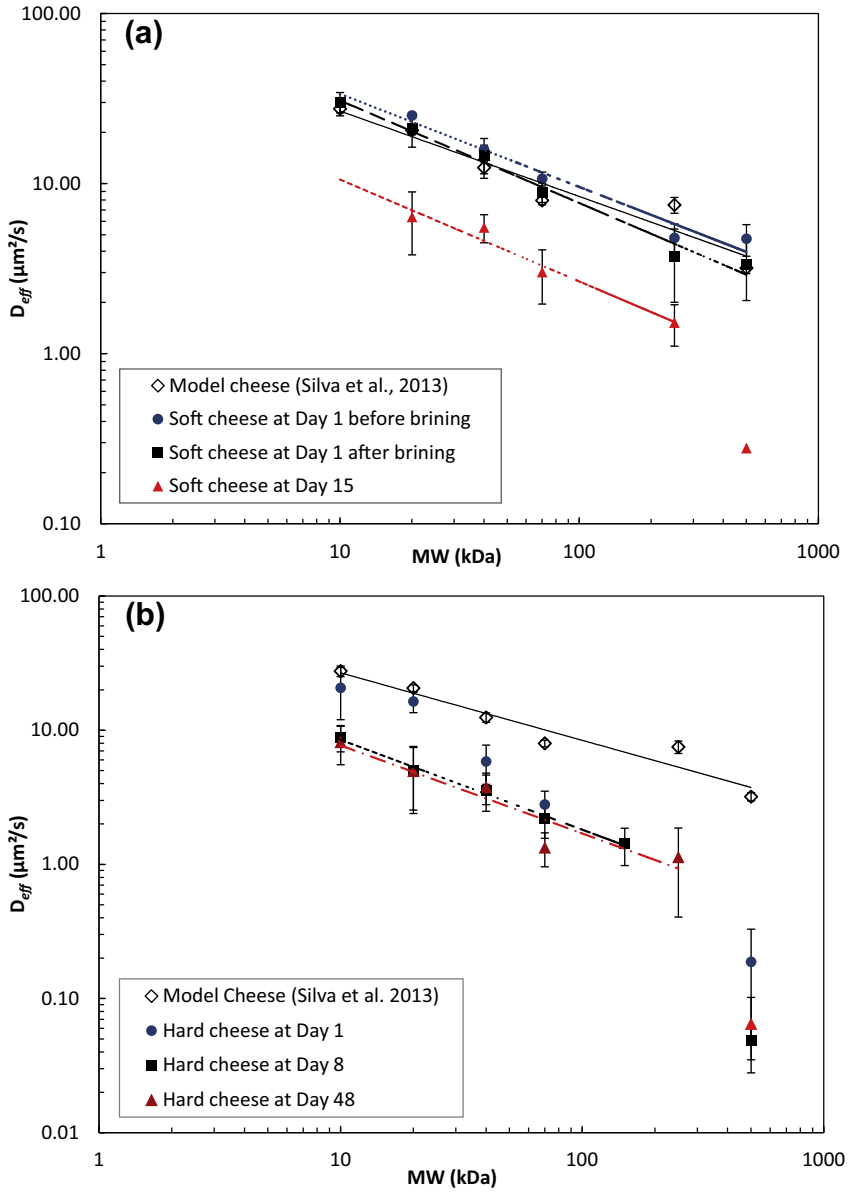

Fig. 2. Logarithmic plots of measured effective diffusion coefficients of fluorescein isothiocyanate (FITC)-dextrans (D_{eff}) as a function of its molecular weight (MW) obtained by FRAP in different types of cheese and ripening times. (a) Model cheese (◇) (data from Silva et al. (2013)) and soft cheese at Day 1 before brining (●), Day 1 after brining (■) and Day 15 (▲). (b) Model cheese (◇) (data from Silva et al. (2013)); hard cheese at Day 1 (●), Day 8 (■) and Day 48 (▲). Lines correspond to the best fit to a power law (Eq. (1)). Error bars show standard deviation of 12 FRAP measurements.

4.1. The "free" water fraction or "free moisture (FM) in non-fat cheese" is a powerful parameter to explain the obstructed diffusion of dextran macromolecules in the protein network of cheese

The effective diffusion coefficients of the dextrans did not depend on the fat content of cheeses, irrespective of the molecular weights. Indeed, the diffusion of such hydrophilic molecules is only expected to occur in the aqueous phase filling the pores of the protein network. Silva et al. (2013) showed that the effective diffusion coefficients of a large range of dextrans (with molecular weights up to 2000 kDa) were reduced in a model cheese by a constant obstruction factor given as 0.42 compared to their respective diffusion coefficient in the aqueous phase alone (D_{eff}/D_{aq}). This obstruction factor is theoretically a function of structural parameters of the protein network, especially (i) the available volume accessible for the diffusion and (ii) the tortuosity of the network (Welti-Chanes, Mujica-Paz, Valdez-Fragoso, & Leon-Cruz, 2003). Based on the power law model (Eq. (1)), because the exponent α remains approximately constant (close to 0.5) for both the model cheese and in the separate aqueous phase, the obstruction factor can also be estimated by calculating the ratio of the constant (A) in the cheese matrix and in the aqueous phase (A_{cheese}/A_{aq}).

In the fresh (unripened) soft cheese at Day 1, the ratio A_{cheese}/A_{aq} was around 0.7 for all dextrans up to the 500 kDa. The interpretation is that the diffusion rates of dextran up to 500 kDa were less hindered (by around 30%) in a fresh cheese curd obtained from a Camembert type technology than in the model cheese (with around 60% obstruction).

The valuation of an obstruction factor to diffusion for dextrans in cheese was also possible during ripening, but in those cases, the ratios were only valid up to the 250 kDa dextran. Noteworthy, in both the soft and hard cheeses at different ages during ripening, the calculated value was relatively constant at around 0.2. In other words, diffusion was restricted by a factor close to 80% for dextrans <250 kDa, and even more for the 500 kDa dextran, irrespective of the cheese technology or the

Table 3
Values of parameters A and α obtained from the best fit of measured effective diffusion coefficients of dextran as function of molecular weights to the power law model (Eq. (1)) for the different cheese samples. R^2 is the coefficient of determination.

Matrix	Day	A	α	R^2
Aqueous phase[a]	–	177	0.5	–
Model cheese[a]	–	75	0.5	–
Soft cheese	1 (before brining)	118	0.5	0.96
	1 (after brining)	123	0.6	0.98
	15	42	0.6[b]	0.96
Hard cheese	1	–	–	–
	8	39[b]	0.6[b]	0.99
	48	34[b]	0.6[b]	0.90

[a] Data from Silva et al. (2013).
[b] Data fitted up to D250.

Table 4
Pearson correlation coefficients between the effective diffusion coefficients of FITC-dextrans (D_{eff}) from 10 to 500 kDa and the variables of the composition of the model, soft and hard cheese (fat, moisture and free moisture in non-fat cheese).

D_{eff}	Fat content (n = 8)	Moisture content (n = 8)	Free moisture in non-fat cheese (n = 8)
D10 (n = 4)	−0.261	0.711	0.779
D20 (n = 8)	−0.254	0.717	0.790
D40 (n = 6)	−0.108	0.754	0.901
D70 (n = 8)	0.004	0.702	0.886
D500 (n = 8)	−0.101	0.752	0.903

n: number of samples used for the statistical test.

ripening time. In parallel, it is noted that the total moisture and free moisture (FM) in non-fat cheese decreased significantly during ripening from Day 1, depending of the cheese type, and these values then remained constant between Day 8 and Day 48 in the case of the hard cheese. As the FM in non-fat cheese value, (i.e. the fraction of water "unbound" to the protein network), correlated well to the effective diffusion coefficients of the dextrans, this parameter appeared to be very suitable in characterizing the fraction of aqueous phase actually available for the diffusion of solutes within the cheese matrix. Therefore, the marked decrease of FM in non-fat cheese for both ripened soft and hard cheeses could be closely linked to the large increase of the effective obstruction to diffusion of dextran observed in both cheese types after ripening, compared to the diffusion rates of the same in the fresh cheese curds. Confocal microscopic observations of the cheese matrices also highlighted that the protein network became effectively much denser after ripening in both types of cheeses. Less aqueous phase was then available for diffusion phenomena in the ripened cheeses, and thus the denser protein network hindered the diffusing solutes much more.

4.2. Modeling diffusion behavior of dextrans across a wide range of sizes allows the study of the cheese microstructure

4.2.1. Soft cheese

It was demonstrated by confocal microscopy that the microstructure of soft cheese curd was highly modified during by the ripening process. In the fresh curd, the diffusion behavior of dextrans (up to 500 kDa) was characteristic by that in an infinite diluted solution (De Gennes, 1979; Silva et al., 2013), implying that flexible macromolecules could diffuse throughout the protein network even without deforming. Silva et al. (2015) used image analysis of TEM micrographs to measure the mean pore size of the protein network as 131 ± 7 nm in their model cheese. In the current study, the effective diffusion coefficients of dextrans were of the same order of magnitude for the soft cheese (at Day 1) as for the cited model cheese. In addition, the dextrans presented the same diffusion behavior in a diluted solution, with a large value for the constant A up to the 500 kDa dextran in both the model and the soft cheese matrices. Therefore, it could reasonably suggested that the pore size of the freshly made soft cheese curd was much greater than the diameter of the largest molecule of dextran tested, (i.e.: 32.4 nm for the D500).

After 15 days of ripening, the large decrease of the effective diffusion coefficient of the biggest dextran molecule (D500) indicated that the characteristic exponent α of the corresponding diffusion regime probably increased. The hypothesis is that a transition in the diffusion behavior of dextran molecules with increasing size occurred between 250 and 500 kDa moving from a dilute regime to a reptation mode. The largest dextran molecule probably had to deform in order to progress through the tight protein network of the cheese (De Gennes, 1979; Tao et al., 2000). Therefore, in the ripened soft cheese, the pore sizes were probably smaller than the diameter of the largest dextran, i.e. around 30 nm. This constricting of the pores could be related both to the manufacturing process of soft cheese and to the physicochemical modifications of the curd throughout the ripening process. When the starter culture was added, the pH of the milk decreased due to the acid-producing bacterial growth. This decrease in pH brought about by the metabolic activity of the starter culture increased the rate of the chymosin activity. These reactions influenced the physico-chemistry of the caseins and led to a strong syneresis of the cheese curd due to the strengthening of the network by more hydrophobic bonds between the proteins. These reactions induced both the tightening of the pores and an increase of the permeability of the fresh curd which caused the syneresis that expelled some of the aqueous phase from the protein network (Mahaut et al., 2000). Finally, the aqueous phase expelled was drained from the fresh curd by gravity via the perforations in the cheese mold. Separated from part of its aqueous phase, the curd grains of the cheese matrix fused together more tightly creating a dense protein network. This important expulsion rate of aqueous phase from the protein network is consistent with the large decrease of the *FM* in non-fat cheese measured between Day 1 and Day 15. Thus, it was concluded that in soft cheese, the tightening of the protein network during ripening caused a large shrinkage of its pore sizes. Moreover, this process was closely linked to both a decrease of the "free" aqueous fraction available in the curd and an increase of the obstruction to the diffusion of dextran molecules.

4.2.2. Hard cheese

A tight protein network was observed by confocal microscopy from the first day of cheese manufacture and then throughout the ripening process (between Days 8 and 48). No significant decrease of FM in non-fat cheese was observed between Day 8 and 48 of ripening, and the diffusion behavior of dextrans up to 250 kDa thus remained similar throughout the ripening process of the hard cheese. Moreover, the large fall in the effective diffusion coefficient of the largest D500 dextran molecule studied meant that a transition from the dilute regime of diffusion to the reptation mode was probably occurring with a solute with MW between that of the two dextrans, D250 and D500. Thus, in the ripened hard cheese, the pore sizes were probably reduced to around 30 nm (or even less) from an early stage of the ripening process. Again, these ideas were consistent with cheese-making technology for hard cheese. Indeed, in a hard cheese, it is known that the microstructure of the protein network is rapidly stiffened during the process of heating and pressing the curd, which cause both an increase and an acceleration of the expulsion of the aqueous phase during the draining process. This activity occurring at an early stage of the process leads to the rapid coalescence of the curd

grains to form a stiff protein network, which then remains tight and dense throughout the subsequent ripening step (Lopez, Camier, & Gassi, 2007).

5. Conclusion

Effective diffusion coefficients for a wide range of dextran molecule sizes in real cheeses were measured by using the FRAP technique. The study related the obstruction to diffusion of solutes in different cheese varieties to their structure and composition parameters. The diffusion rates of dextrans mainly depended on the fraction of "free" aqueous phase available within the cheese, which could be measured by a parameter referred to as the free moisture (FM) in non-fat cheese. This parameter was closely linked to the cheese-making technology and the ripening stage of the cheese samples. Diffusion behaviors of the dextrans were also affected by the hydrodynamic interactions between the diffusing solute molecules and the protein network of the developing cheese. A tighter protein network seemed to require a deformation of those flexible macromolecules with a high molecular weight (>250 kDa), which therefore adopted a reptation behavior to diffuse through the pores of the network. Modeling the diffusion behavior of dextrans over a wide range of sizes allowed the study features of the cheese microstructure such as the pore size of the protein network. It was possible to detect microstructural changes during the ripening of different types of cheeses. The FRAP procedure appeared to be a powerful technique to explore both diffusion phenomena in heterogeneous food matrices and their microstructure. The next step would be the study of diffusion behavior of other solutes such as proteins (including enzymes), with different physicochemical properties (compared to dextrans), in order to complete the understanding of the behavior of diffusing solutes in cheese.

Acknowledgements

The contribution of funding from the European Union Seventh Framework Programme (FP7/2007-2013) under Grant agreement n°289397 (TeRiFiQ project) is gratefully acknowledged. More specifically, the authors would also like to thank Anne Dolivet for her technical help with the water desorption measurements. Furthermore, the authors gratefully acknowledge the help of Jean-Yves Gassi and Valérie Gagnaire with respect to the production of the soft and hard cheeses used.

Appendix A. Supplementary data

Supplementary data associated with this article can be found, in the online version, at http://dx.doi.org/10.1016/j.foodchem.2015.07.053.

References

Aly, S., Floury, J., Famelart, M.-H., Madec, M.-N., Dupont, D., Le Gouar, Y., et al. (2011). Nisin quantification by ELISA allows the modelling of its apparent diffusion coefficient in model cheeses. *Journal of Agricultural and Food Chemistry, 59*, 9484–9490.

Bouchoux, A., Gésan-Guiziou, G., Pérez, J., & Cabane, B. (2010). How to squeeze a sponge: Casein micelles under osmotic stress, a SAS study. *Biophysical Journal, 99*, 3754–3762.

Braga, J., Desterro, J. M. P., & Carmo-Fonseca, M. (2004). Intracellular macromolecular mobility measured by fluorescence recovery after photobleaching with confocal laser scanning microscopes. *Molecular Biology of the Cell, 15*, 4749–4760.

De Gennes, P. G. (1979). Brownian motions of flexible polymer chains. *Nature, 282*, 367–370.

Favre, E., Leonard, M., Laurent, A., & Dellacherie, E. (2001). Diffusion of polyethyleneglycols in calcium alginate hydrogels. *Colloids and Surfaces A: Physicochemical and Engineering Aspects, 194*, 197–206.

Floury, J., Jeanson, S., Aly, S., & Lortal, S. (2010). Determination of the diffusion coefficients of small solutes in cheese: A review. *Dairy Science and Technology, 90*, 477–508.

Floury, J., Madec, M.-N., Waharte, F., Jeanson, S., & Lortal, S. (2012). First assessment of diffusion coefficients in model cheese by fluorescence recovery after photobleaching (FRAP). *Food Chemistry, 133*, 551–556.

IDF/FIL. (1986). *Fromage et fromage fondu: détermination de la teneur en matière grasse, standard 5B*. Brussels, Belgium: International Dairy Federation.

IDF/FIL. (1987). *Lait, crème et lait concentré non sucré, détermination de la matière sèche, standard 21B*. Brussels, Belgium: International Dairy Federation.

Jeanson, S., Chadœuf, J., Madec, M. N., Aly, S., Floury, J., Brocklehurst, T. F., et al. (2011). Spatial distribution of bacterial colonies in a model cheese. *Applied and Environmental Microbiology, 77*, 1493–1500.

Lopez, C., Camier, B., & Gassi, J.-Y. (2007). Development of the milk fat microstructure during the manufacture and ripening of Emmental cheese observed by confocal laser scanning microscopy. *International Dairy Journal, 17*, 235–247.

Mahaut M., Jeantet R., Brulé G. (2000). Initiation à la technologie fromagère (1st ed.). Lavoisier, Tec et Doc, Paris, 194 p.

McSweeney, P. L. H. (2004). Biochemistry of cheese ripening. *International Journal of Dairy Technology, 57*, 127–144.

Schuck, P., Dolivet, A., Méjean, S., Zhu, P., Blanchard, E., & Jeantet, R. (2009). Drying by desorption: A tool to determine spray drying parameters. *Journal of Food Engineering, 94*, 199–204.

Silva, J. V. C., Legland, D., Cauty, C., Kolotuev, I., & Floury, J. (2015). Characterization of the microstructure of dairy systems using automated image analysis. *Food Hydrocolloids, 44*, 360–371.

Silva, J. V. C., Peixoto, P. D. S., Lortal, S., & Floury, J. (2013). Transport phenomena in a model cheese: The influence of the charge and shape of solutes on diffusion. *Journal of Dairy Science, 96*, 6186–6198.

Tao, H., Lodge, T. P., & von Meerwall, E. D. (2000). Diffusivity and viscosity of concentrated hydrogenated polybutadiene solutions. *Macromolecules, 33*, 1747–1758.

Ulve, V. M., Monnet, C., Valence, F., Fauquant, J., Falentin, H., & Lortal, S. (2008). RNA extraction from cheese for analysis of in situ gene expression of *Lactococcus lactis*. *Journal of Applied Microbiology, 105*, 1327–1333.

Welti-Chanes, J., Mujica-Paz, H., Valdez-Fragoso, A., & Leon-Cruz, R. (2003). Fundamentals of mass transport. In J. Welti-Chanes, J. F. Vélez-Ruiz, & G. V. Barbosa-Canovas (Eds.), *Transport Phenomena in FoodProcessing* (pp. 3–23). Boca Raton: CRC Press.